Weaver, P.P.E., Schmincke, H.-U., Firth, J.V., and Duffield, W. (Eds.), 1998
Proceedings of the Ocean Drilling Program, Scientific Results, Vol. 157

21. ORGANIC MATTER IN NEOGENE SEDIMENTS OF THE SOUTHERN CANARY CHANNEL, CANARY ISLANDS (SITES 955 AND 956)[1]

Ralf Littke,[2,3] Andreas Lückge,[2,4] and Heinz Wilkes[2]

ABSTRACT

Detailed organic geochemical and organic petrologic investigations were performed on sediment samples from Site 955, southeast of Gran Canaria. In addition, some basic data were assembled for Sites 956 and 954, southwest and northeast, respectively, of Gran Canaria. These data reveal that the organic matter is composed of a complex mixture of marine and terrestrial-derived material. The rate of preservation of the organic matter is surprisingly high, and, accordingly, hydrogen index values calculated from Rock-Eval pyrolysis data are as high as those in the upwelling sediments along the continental slope off northwest Africa. Part of the organic matter is preserved in response to mass and turbidity transport processes, leading to low rates of aerobic degradation in the rapidly buried sediments. None of the assembled organic geochemical and organic petrologic data—not even from the deeper samples—indicated an anomalously enhanced level of organic matter maturation in the vicinity of the Canary hot spot.

INTRODUCTION

During the past decades, investigations of deep-sea sediments drilled in the framework of the international Deep Sea Drilling Project and its successor, the Ocean Drilling Program, led to an enhanced understanding of organic matter deposition and preservation in the oceans. For instance, it has been established during this period that typical modern deep-sea sediments contain <0.3% organic carbon, but that organic carbon concentrations were much higher during several Cretaceous periods (e.g., the Aptian through Albian and Cenomanian through Turonian; Schlanger and Jenkyns, 1976; Stein et al., 1986). In recent times, sediments with organic carbon content >1% have usually been restricted to continental slope environments or their vicinity. Stein and Littke (1990:42) summarized that "the deposition of these carbon-rich sediments requires special environmental conditions such as (1) high surface-water productivity, (2) increased preservation of organic matter, (3) enhanced supply of terrigenous organic matter, and (4) rapid burial of organic matter." Over the last several years, the relative importance of these factors has become a matter of intense scientific debate, especially for oceanic settings (Müller and Suess, 1979; Pedersen and Calvert, 1990; Demaison, 1991).

It was one of our objectives to study organic matter accumulation and preservation in sediments at ODP Sites 954, 955, and 956, situated south of Gran Canaria and Tenerife, where deposition is influenced significantly by the northwest African continental margin as well as by the erosion of the volcanoes on the Canary Islands (Schmincke, Weaver, Firth, et al., 1995). It was of special interest to investigate whether redistribution of organic carbon–rich sediments from the upwelling zone off the shores of Morocco and Mauretania have an impact on the deposition, and to what extent material derived from higher land plants or from the erosion of older and mature African sedimentary rocks contributed to the sedimentary organic matter at Sites 955 and 956. A comparable situation was already observed off the southwest shore of Africa, where organic matter–rich upwelling sediments that accumulated along the continental margin were slumped into the deep ocean (Meyers, 1992). To study whether similar sedimentation processes led to the deposition of hydrogen-rich sedimentary organic matter at Sites 955 and 956, geochemical and petrographical data from the latter sites will be compared with data from Sites 658 and 659 at or near the upwelling zone of northwest Africa (Fig. 1), for which a good database on organic matter quantity and quality already exists (Ruddiman, Sarnthein, Baldauf, et al., 1988; Stein et al., 1989).

Furthermore, earlier studies on organic matter maturation in the vicinity of volcanoes showed that very high heat flows had occurred during volcanic activity, which had affected the organic matter to a great extent (e.g., Sachsenhofer and Littke, 1993). As the recent Canary hot spot affects a rather large oceanic area compared to other hot spots (Schmincke, Weaver, Firth, et al., 1995), it seemed possible that high heat flows and elevated temperatures also led to organic matter maturation in the deepest sediments drilled at Sites 954, 955, and 956. Maturation effects for deep-sea sediments drilled at rather shallow depths were established earlier for areas of high volcanic activity and high heat flow (e.g., at the triple junction off the shore of Chile; Kvenvolden et al., 1995). Therefore, the second objective of this study was to investigate whether high heat flows affected the organic matter maturation in the deepest sediments drilled at Sites 955 and 956.

Two of the three sites, 955 and 956, are situated in the southern Canary Channel south of the island Gran Canaria (Fig. 1). Site 955 is the more landward of the two locations, situated 55 km southeast of Gran Canaria, 110 km southwest of Fuerteventura, and 125 km west of the African continental margin. The drill site is located in a fairly flat area at ~2860 m water depth, and drilling reached a final depth of 599 meters below seafloor (mbsf). Site 956 is situated 60 km southwest of Gran Canaria, 65 km southeast of Tenerife, and ~200 km west of the African continental margin. Water depth at Site 956 is ~3440 m, and drilling was terminated at 704 mbsf. Lithologically, the sedimentary successions at both sites are composed mainly of hemipelagic, fine-grained nannofossil oozes with interbedded coarse-grained volcaniclastic and siliciclastic material. Some of the volcaniclastic layers can be correlated to the magmatic phases of Gran Canaria and

[1]Weaver, P.P.E., Schmincke, H.-U., Firth, J.V., and Duffield, W. (Eds.), 1998. *Proc. ODP, Sci. Results*, 157: College Station, TX (Ocean Drilling Program).

[2]Institut für Erdöl und Organische Geochemie (ICG-4), Forschungszentrum Jülich GmbH, 52425 Jülich, Federal Republic of Germany.

[3]Present address: Institute of Geology and Geochemistry of Petroleum and Coal, Aachen University of Technology, Lochnerstrasse 4-20, 52056 Aachen, Federal Republic of Germany. littke@lek.rwth-aachen.de

[4]Present address: BGR, Stilleweg 2, 30655 Hannover, Federal Republic of Germany.

Prior Chapter Contents Next Chapter

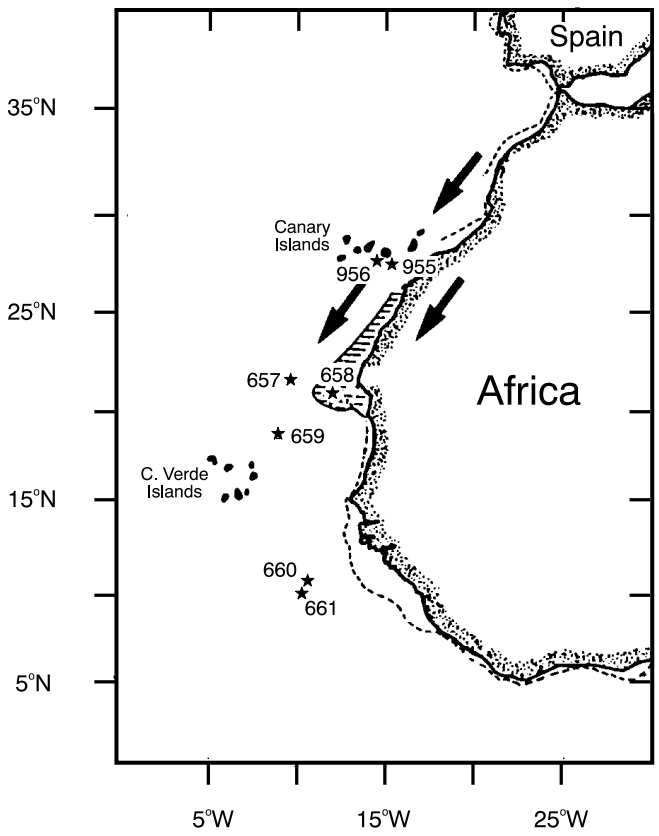

Figure 1. Location map of ODP Sites 955 and 956, drilled south of Canary Islands during Leg 157, and of Sites 657 to 661, drilled during Leg 108. The hatched pattern marks the upwelling area off northwest Africa, and the arrows indicate northeasterly trade winds.

Tenerife (Schmincke, Weaver, Firth, et al., 1995). Stratigraphically, the sedimentary successions range from Quaternary to middle Miocene at both sites. It is expected that sedimentation at these sites was influenced by erosion processes along the African continental margin (Schmincke, Weaver, Firth, et al., 1995). In contrast, sediments at Site 954, which was drilled 45 km northeast of Gran Canaria, are assumed to be less affected by the northwest African continental margin. Water depth at this site was ~3485 m. A total of 446 m of siliciclastic, carbonatic, and volcaniclastic sediments were drilled at this location. At Site 954, the age of these deposits ranges from middle Miocene to Holocene.

METHODS

Total carbon (TC) and sulfur concentrations were measured by the combustion of dried and ground sediment with a LECO IR-112 analyzer. The same instrument was used for total organic carbon (TOC) determination after removal of carbonate with hydrochloric acid (25%). Carbonate-carbon concentrations were determined by difference as $C_{inorg} = TC - C_{org}$. Calcium carbonate percentages were calculated as $C_{inorg} \times 8.333$. A different, coulometric method was used aboard the *JOIDES Resolution* (Schmincke, Weaver, Firth, et al., 1995). According to Stein et al. (1988) and Littke et al. (1995), the results obtained by these different analytical approaches are almost identical. Therefore, carbonate-carbon and C_{org} data sets from both methods are combined in this contribution without any numerical correction. Additional elemental analyses were carried out on kerogen concentrates. These concentrates were prepared by subsequent dissolution of carbonates and silicates in hydrochloric and hydrofluoric acid, following the procedures described by Durand (1980). The residue mainly contains organic matter and pyrite. The elemental composition of the kerogen concentrates was determined using the same analytical devices as described above for chemically untreated sediment ("whole rock").

Rock-Eval pyrolysis was performed with a DELSI Rock-Eval II instrument on a limited number of samples, which were selected on the basis of organic carbon percentages and on kerogen concentrates. The procedure is described in detail in Espitalié et al. (1977) and in Tissot and Welte (1984). Rock-Eval parameters used in this contribution are hydrogen index (HI) values (milligrams of hydrocarbon [HC]-equivalents per gram of C_{org}), oxygen index (OI) values (milligrams of CO_2 per gram of C_{org}), and T_{max} values (i.e., temperatures of maximum pyrolysis yield).

Whereas Rock-Eval pyrolysis measures the total amounts of volatile organic compounds generated during the heating of organic matter in an oxygen-free atmosphere, pyrolysis, coupled with gas chromatography (Py-GC), provides molecular information on the generated products. Py-GC was performed on kerogen concentrates on a Hewlett Packard 5731A gas chromatograph equipped with an HP-1 fused silica capillary column (Hewlett Packard) 25 m long, with a 0.31-mm inner diameter and a 0.52-µm film thickness. The samples were filled in a 30 mm glass tube and were heated in a flow of helium to 300°C. This temperature was kept constant for 5 min. The samples were then heated up to 600°C at 50°C/min, and the products released in this temperature range were collected in a trap cooled by liquid nitrogen. After the experiment, the trap was heated and the pyrolysis products were analyzed in the gas chromatograph described above, with helium used as the carrier gas. The oven temperature was programmed from 40°C to 320°C at 5°C/min. Alkanes, alkenes, alkylbenzenes, alkylthiophenes, and alkyl-pyrroles were quantified by external standardization.

For microscopic studies, sediment samples and kerogen concentrates were embedded in a resin, ground flat, and polished. The polished blocks were investigated in incident white light and in an incident light fluorescence mode at high magnifications (300 to 1000×). Because the typical maceral classification used for coals (Stach, 1982) is not very useful for deep marine sediments, only four groups of organic particles were differentiated: (1) vitrinites, (2) inertinites and resedimented organic particles derived from mature to overmature rocks, (3) structured marine particles (alginites and remains of dinoflagellates), and (4) unstructured, probably marine-derived, organic matter (see Littke and Sachsenhofer, 1994). Countings of macerals were performed on 12 samples from Site 955 in a two-scan mode, first in reflected white light, then in fluorescent light excited by ultraviolet (UV) and violet light. For maturity assessment, vitrinite reflectance was measured on some of the deeper samples from both sites. Vitrinite reflectance measurements followed standard procedures (Stach, 1982) and were performed on particles larger than 10 µm in oil immersion at a wavelength of 546 nm.

For the analysis of nonaromatic hydrocarbons, nine selected samples were dried at 45°C and extracted by flow-blending (Radke et al., 1978) with dichloromethane-methanol (99:1). The extracts were separated into nonaromatic hydrocarbons, aromatic hydrocarbons, and heterocompounds by medium-pressure liquid chromatography (Radke et al., 1980). For the analysis of fatty acids, six selected samples were freeze-dried and subsequently extracted by flow-blending with an azeotropic mixture of chloroform, methanol, and acetone. The extracts were fractionated by polarity chromatography. During this procedure, the free fatty acids were isolated using a column containing silica gel impregnated with potassium hydroxide, from which the acids were eluted with a solution of formic acid in dichloromethane (1% by volume). The free fatty acids were methylated with diazomethane before gas chromatographic analysis.

Gas chromatography of nonaromatic hydrocarbons was performed on a Hewlett Packard 5890B instrument equipped with an on-column injector and a flame ionization detector. Hydrogen was used as the carrier gas. The gas chromatograph was equipped with an Ultra II fused silica capillary column (Hewlett Packard) 50 m in length, with a 0.2-mm inner diameter and a 0.33-µm film thickness. The oven temperature was programmed from 90°C (hold time 4 min) to 310°C (hold time 50 min) at 3°C/min.

For gas chromatography-mass spectrometry (GC-MS), a Finnigan MAT 95SQ mass spectrometer was used, which was coupled to a Hewlett Packard 5890B gas chromatograph. The mass spectrometer was operated in electron ionization mode at an ionization energy of 70 eV and a source temperature of 260°C. Full scan mass spectra were recorded over the mass range of 35 to 800 da at a cycle time of 1.2 s. The gas chromatograph was equipped with a temperature-programmable injection system (Gerstel KAS 3) and a BPX5 fused silica capillary column (SGE) 50 m in length, with a 0.22-mm inner diameter and a 0.33-µm film thickness. Helium was used as the carrier gas. For GC-MS of nonaromatic hydrocarbons, the oven temperature was programmed from 60°C to 340°C (hold time 8 min) at 3°C/min. For GC-MS of fatty acid methyl esters, the oven temperature was programmed from 110°C to 340°C (hold time 13 min) at 3°C/min.

Mass accumulation rates of organic carbon (AROC) were calculated according to van Andel et al. (1975) using the physical properties and sedimentation rate data of Schmincke, Weaver, Firth, et al. (1995) as

$$AROC = (C_{org}/100) \cdot SR \cdot (WBD - 1.026\ Po/100),$$

where *AROC* is the mass accumulation rate (g/m^2/a), *SR* is the average sedimentation rate (m/a), *WBD* is the wet bulk density (kg m^{-3}), and *Po* is the porosity (%).

RESULTS AND DISCUSSION

Quantity of Organic Matter

Shore-based measurements of organic carbon percentages were carried out on 49 samples from Site 955 and on nine samples from Site 956. These sample sets cover the depth range between 0.2 and 594 mbsf and between 17 and 373 mbsf, respectively. In addition, eight samples from Site 954, drilled northeast of Gran Canaria, were analyzed for their organic carbon concentrations.

At Site 954, organic carbon concentrations varied between 0.07% and 0.13% without any significant depth trend. These values are even lower than those reported for average deep-sea sediments, which are as low as ~0.2% (McIver, 1975). The results of the shore-based measurements agree well with the values measured aboard the *JOIDES Resolution*, which range from 0% to 0.22%.

At Site 955, organic carbon concentrations ranged from 0.15% to 2.14% (Table 1; Fig. 2). The highest values are restricted to the uppermost 90 m of the sedimentary sequence (i.e., about the upper third of lithologic Unit I; Schmincke, Weaver, Firth, et al., 1995). Stratigraphically, these units belong to the Pleistocene and uppermost Pliocene. Below this sequence, organic carbon concentrations rarely exceed 0.5% but are usually >0.2%. Thus, the average concentration of sedimentary organic carbon at this site significantly exceeds the average value for deep-sea sediments (0.2%; McIver, 1975). The highest values are recorded for the interval between ~38 and 50 mbsf, which is also characterized by a minimum number of sand units (Schmincke, Weaver, Firth, et al., 1995).

Organic carbon concentrations of sediments from Site 956 range from 0.16% to 1.38% (Table 1). The highest values occur in the upper part of the sequence, especially in the upper 60 mbsf (Fig. 3), with a maximum value at ~17 mbsf. The upper 60 m of the sedimentary sequence are clayey nannofossil oozes with interlayered sand and ash layers (Schmincke, Weaver, Firth, et al., 1995) of Pleistocene age. The Pliocene and Miocene sequences below are enriched in volcanogenic sediments and contain only ~0.2% organic carbon.

Table 1. Carbonate, organic carbon, and total sulfur concentrations (weight percent) in samples from Sites 955 and 956.

Core, section, interval (cm)	Depth (mbsf)	TOC (%)	S (%)	$CaCO_3$ (%)	TOC/S (%)
157-955A-					
1H-1, 17-21	0.17	0.31	0.13	47.4	2.4
1H-2, 81-85	2.41	0.91	0.39	50.9	2.3
1H-4, 74-78	5.24	0.52	0.42	50.6	1.2
2H-2, 12-18	9.72	0.89	0.72	46.0	1.2
2H-2, 122-128	10.82	0.76	0.44	57.1	1.7
2H-6, 117-123	16.77	0.53	0.44	57.1	1.2
3H-3, 51-57	21.11	0.47	0.38	61.2	1.2
3H-5, 83-89	24.43	0.48	0.24	50.3	2.0
3H-7, 55-61	27.15	1.22	0.66	58.0	1.9
4H-2, 58-64	29.18	0.29	0.07	79.6	4.1
4H-4, 31-37	31.91	0.54	0.36	9.9	1.8
4H-6, 89-95	35.49	0.52	0.22	61.7	2.4
5H-2, 46-48	38.56	2.14	1.61	29.7	1.3
5H-5, 43-45	43.04	0.74	0.34	51.9	2.2
6H-2, 70-73	48.30	1.13	0.72	49.1	1.6
6H-4, 30-33	50.90	1.29	0.84	49.8	1.5
7H-2, 58-61	57.69	0.37	0.32	38.4	1.2
7H-6, 126-129	64.36	0.41	0.59	54.9	0.7
8H-6, 130-133	73.90	1.41	1.28	34.7	1.1
10H-2, 96-100	86.66	1.30	0.94	50.2	1.4
13H-1, 55-58	113.15	0.41	0.43	52.9	1.0
13H-6, 104-107	121.14	0.49	0.36	51.8	1.4
14H-4, 56-59	127.16	0.32	0.69	61.1	0.5
15H-5, 98-101	138.58	0.31	0.64	57.7	0.5
16H-7, 47-50	150.62	0.36	0.66	48.7	0.6
17H-6, 39-42	158.49	0.51	1.31	41.0	0.4
18H-5, 95-101	167.05	0.35	0.26	52.1	1.3
19X-6, 71-75	177.11	0.57	0.46	27.0	1.2
20X-1, 95-99	177.35	0.56	0.53	4.8	1.1
30X-1, 88-91	273.78	0.21	0.35	41.0	0.6
33X-4, 80-83	306.50	0.23	0.16	30.2	1.4
35X-3, 110-113	323.28	0.22	0.27	23.0	0.8
36X-5, 60-64	336.70	0.25	0.23	29.0	1.1
37X-1, 96-99	340.56	0.25	0.22	22.5	1.1
38X-6, 116-123	357.76	0.2		35.7	
39X-4, 24-27	363.44	0.2	0.22	5.6	1.0
40X-6, 70-73	376.50	0.24		20.7	
41X-5, 17-21	384.07	0.15	0.14	30.3	1.1
42X-2, 81-85	389.81	0.27		21.7	
45X-2, 118-121	419.18	0.21	0.21	24.3	1.0
49X-3, 136-139	459.56	0.24		22.2	
51X-1, 33-36	474.73	0.34	0.77	14.2	0.4
55X-3, 6-9	515.96	0.34		4.1	
56X-3, 10-13	525.5	0.26	0.34	12.2	0.8
58X-5, 30-34	547.90	0.29		27.4	
60X-3, 70-76	564.60	0.4	0.5	20.5	0.8
61X-1, 23-26	570.73	0.29		29.6	
62X-7, 27-29	588.09	0.29	0.36	20.8	0.8
63X-4, 26-32	594.26	0.2		22.0	
157-956A-					
3H-2, 26-28	17.36	1.38	0.47	46.0	2.9
5H-5, 34-37	40.94	0.2		44.8	
8H-2, 61-64	65.21	0.4	0.44	51.4	0.9
11H-3, 79-83	95.39	0.61		34.7	
15H-5, 96-99	136.56	0.4	0.23	44.5	1.7
157-956B-					
5R-5, 36-39	201.66	0.18	0.2	54.4	0.9
16R-5, 111-115	308.41	0.16	0.08	47.6	2.0
20R-6, 107-113	346.57	0.21	0.12	7.0	2.1
23R-4, 44-47	373.34	0.22	0.14	24.2	1.6

Thus, it can be summarized that organic carbon concentrations are much higher at the sites south of the Canaries than at Site 954, located northeast of Gran Canaria. Furthermore, at Site 955, closest to the continent, organic matter is more abundant than at the more distant Site 956 (Table 2). Stratigraphically, the Pleistocene sediments are more enriched in organic carbon, whereas the Pliocene and Miocene sequences contain, on average, not much more than ~0.2% C_{org}, which is typical of deep-sea sediments (McIver, 1975).

Mass accumulation rates of organic carbon were calculated only for the Pleistocene and Pliocene intervals at Sites 955 and 956 (Table 2). The average values vary between 0.1 and 0.5 g C/(m^{2}a) and indicate that the masses of organic matter deposited during the Pliocene

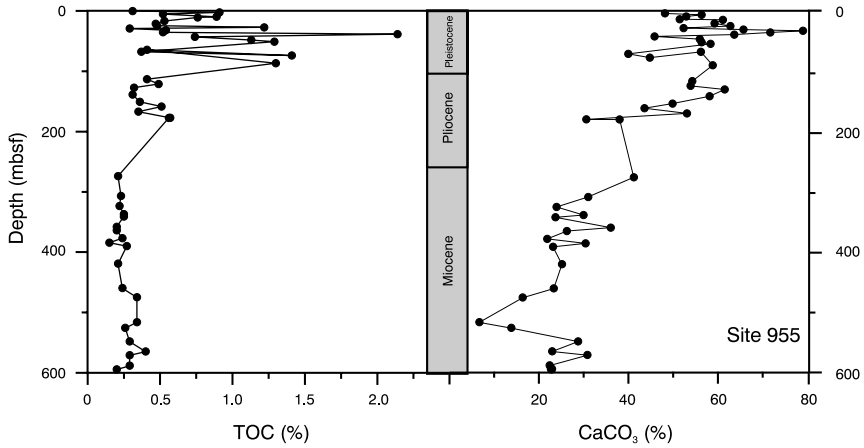

Figure 2. Depth profiles of organic carbon and carbonate for Site 955. Only the onshore measurements are shown, which agree well with the data measured aboard the *JOIDES Resolution* (Schmincke, Weaver, Firth, et al., 1995).

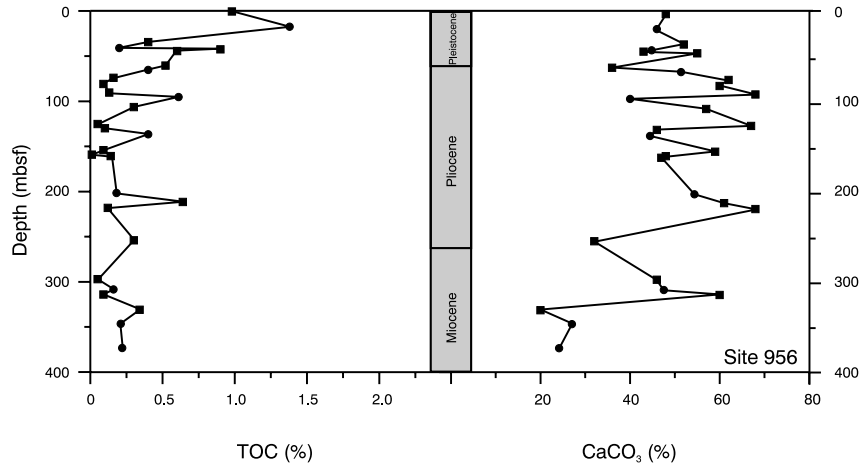

Figure 3. Depth profiles of organic carbon and carbonate for Site 956. Circles = onshore measurements, and squares = measurements made on board the *JOIDES Resolution* (Schmincke, Weaver, Firth, et al., 1995).

Table 2. Average weight percentages of the Pleistocene and Pliocene sections, Sites 955 and 956.

	TOC (%)	S (%)	$CaCO_3$ (%)	AROC (g C/m^2/a)	ARCaCO$_3$ (g $CaCO_3$/m^2/a)
955A Pleistocene	0.79	0.53	52.5	0.5	35
955A Pliocene	0.53	0.62	47.7	0.1	9
956A Pleistocene	0.67	0.33	47.0	0.15	11
956B Pliocene	0.22	0.08	55.9	-	-

Note: See Schmincke, Weaver, Firth, et al., 1995.

are smaller than those deposited during the Pleistocene. Thus, lower organic matter supply and/or preservation, not dilution by mineral matter, caused the lower organic carbon concentrations in the late Tertiary as compared with the Quaternary. This conclusion has, however, to be taken as an estimation because sedimentation rates for the Pliocene are doubtful (see Schmincke, Weaver, Firth, et al., 1995).

The mass accumulation rates of organic matter are lower than those established for Neogene upwelling sediments, which also show higher concentrations of organic carbon (caused by less dilution by mineral matter). For example, the well-known upwelling sediments off the shores of Peru and Oman contain, on average, ~4% organic carbon, and the mass accumulation rates average at 3 to 4 g C/(m^{2}a) (Lückge et al., 1996). For the upwelling Site 658 off the shore of northwest Africa, which is situated close to the Canary sites investigated here, values of ~2 g C/(m^{2}a) were published (Stein and Littke, 1990). If these values are compared with accumulation rates of organic carbon determined for distal open marine sediments (e.g., Littke et al., 1991), the Canary values are higher by a factor of ~100.

Carbonate and Sulfur Contents

For Sites 955 and 956, the contents of carbonate are documented in Table 1 and are summarized for some stratigraphic intervals in Table 2. Carbonate contents mainly reflect the relative abundance of calcareous nannofossils and foraminifers, which stem from biogenic carbonate production at locations close to the site of deposition. In contrast, most of the noncarbonate within the sediments are derived from erosion processes or volcanic eruptions such as those on the Canaries.

At Site 955, carbonate percentages tend to increase from bottom to top (Fig. 2). Most values scatter ~20% between 300 and 525 mbsf (i.e., in the upper and middle Miocene) and are >40% in the uppermost Miocene, Pliocene, and Pleistocene sequences above. Accumulation rates for carbonate are at 9 g $CaCO_3$/(m^{2}a) in the Pliocene sequence and at 35 g $CaCO_3$/(m^{2}a) in the Pleistocene sequence (Table 2). The upward increasing carbonate accumulation reflects the overall increasing sedimentation rates.

Similarly, there is a tendency for carbonate content to increase with decreasing age and depth below seafloor at Site 956 (Fig. 3). Again, the lowest values are recorded for the upper and middle Miocene sequences (~25%, deeper than 315 mbsf), whereas many of the measured carbonate concentrations in the uppermost Miocene, Pliocene, and Pleistocene sequences above are on the order of 50% to 60%. Carbonate concentrations are similar to those measured at Site

955. Carbonate accumulation rates are at ~11 g $CaCO_3/(m^2a)$ in the Pleistocene sequence.

Sulfur in marine sediments is usually the product of early diagenetic formation of pyrite or, less commonly, organic sulfur. This formation is triggered by sulfate-reducing bacteria that feed mainly on freshly deposited, sedimentary organic matter. As long as sulfate in pore water and metabolizable organic matter are available, sulfate reduction can proceed. Berner (1970, 1984) found an empirical relationship between sulfur and organic carbon content, which is typical of most marine sediments deposited under aerobic conditions. This relationship is shown in Figure 4, together with the data for the samples from Sites 955 and 956 (also see Table 1). Most samples plot above the trend line defined by Berner (1970, 1984).

A clear deviation from this trend was mainly established for samples from Site 955 at 125 to 165 mbsf, where sulfur to organic carbon ratios >1 were found. This part of the sedimentary sequence is characterized by the most intense slumping recorded for this site (Schmincke, Weaver, Firth, et al., 1995). Thus, the sediments may contain some pyrite that was not formed in situ but was transported by mass or turbidity flow to the site of deposition. The sum of inherited and newly formed pyrite may explain the excess sulfur in this interval. Another possible explanation would be the assumption of anoxic bottom-water conditions, but this seems less likely in view of the bioturbation and organic matter quantity and quality.

Quality of Organic Matter

The characterization of the insoluble organic matter (kerogen) was performed by means of Rock-Eval pyrolysis, pyrolysis-gas chromatography, and microscopy for sediments drilled at Sites 955 and 956. Parameters determined by Rock-Eval pyrolysis are HI and OI values, which are plotted in Figure 5. HI values vary between 150 and 240 mg HC/g C_{org} for whole-rock samples and between 150 and 320 for kerogen concentrates (Table 3). Samples from the upper 100 m of the sedimentary succession at both sites tend to have higher HI values than those from below 150 m. The HI values were determined for the samples richest in organic carbon. According to our experience, smaller values can be expected for the samples of the studied sequence that are leaner in organic carbon. The differences between HI values of whole-rock and kerogen concentrate samples (Fig. 5) are caused by the storage of hydrocarbons on mineral surfaces in whole-rock samples, as already described by Katz (1983). OI values vary between 60 and 110 mg CO_2/g C_{org} and are unreliable (because of carbonate destruction) for whole-rock samples (Fig. 5).

If compared with the commonly used trend lines for oil-prone type I and II kerogens and gas-prone type III kerogens, the values established for Sites 955 and 956 clearly fall between the trend lines for type II and III kerogens. This observation is somewhat surprising because most deep-sea sediments contain a hydrogen-poor type III kerogen. The organic matter from Sites 955 and 956 is, however, almost as hydrogen rich as the sedimentary organic matter from the upwelling-related sediments at Site 658 (Stein et al., 1989), which is located between the Canary and Cape Verde Islands, ~600 km south of Site 956. The range of HI values for Site 658 is also plotted in Figure 5.

Further insight into the nature of organic matter was obtained by the identification of pyrolysis products. The gas chromatograms are rather similar for the eight samples from Sites 955 and 956 investigated by this technique and are characterized by high concentrations of both gaseous compounds with <6 carbon atoms and higher molecular-weight compounds. In the latter group, hydrocarbons clearly predominate over nitrogen, sulfur, and oxygen (NSO) compounds. The relative concentration of NSO compounds and of aromatic and nonaromatic hydrocarbons are shown in Table 3 and in Figure 6. At Site 955, the relative amounts of nonaromatic hydrocarbons are nearly constant. With the exception of one Miocene sample (40%), the values range between 45% and 48%. The aromatic hydrocarbon percentages are slightly higher in value in the deeper section of this site. The average concentration in the Pleistocene and upper Miocene sediments is 37%, and in the middle Miocene sequence, it averages 43%. The relative concentrations of thiophenes show only minor variations over the entire sequence. The percentages vary without a clear trend from 7% to 10%. The concentrations of pyrroles decrease with increasing depth. At the top of the sequence, the amount of pyrrols is 9%, whereas at the bottom, a value of 3% was observed.

If compared with the relative concentrations of these compounds in upwelling sediments (see Fig. 6 [hatched field]), the percentages of the heterocompounds are distinctly lower at Site 955, whereas per-

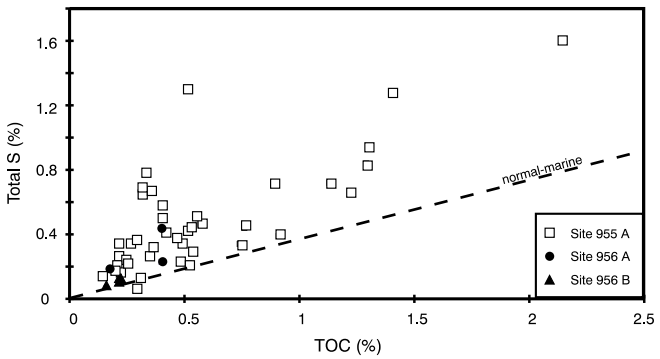

Figure 4. Total sulfur and organic carbon weight percentages for samples from Sites 955 and 956. Most samples plot slightly above the trend line defined by Berner (1984; dashed line in the figure) for marine sediments deposited under aerobic conditions.

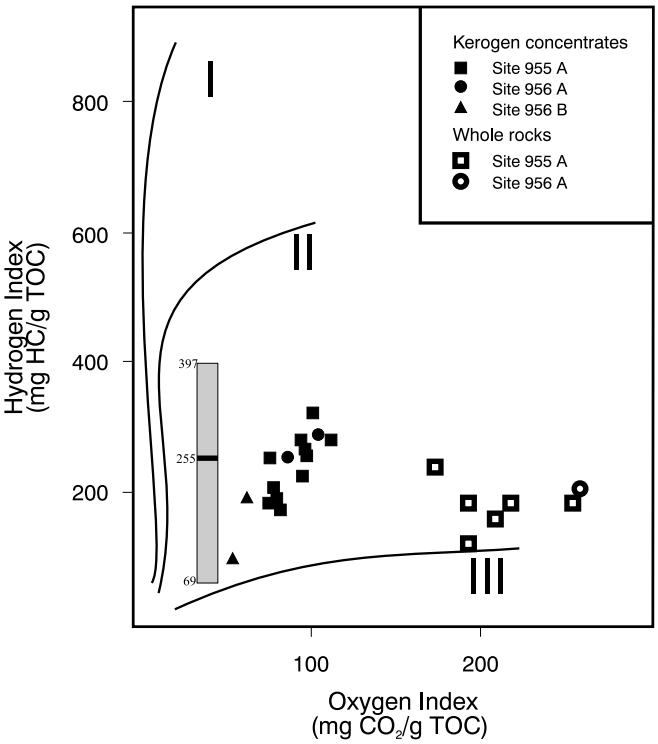

Figure 5. HI and OI values determined on sediments (open symbols) and kerogen concentrates (solid symbols) from Sites 955 and 956. The bar along the vertical axis represents the range of HI values established for the sediments below the upwelling area of northwest Africa (Site 658; Stein et al., 1989).

Table 3. Results of quantification of individual compounds obtained by pyrolysis-gas chromatography and hydrogen index of kerogen concentrates for Sites 955 and 956.

Core, section, interval (cm)	Depth (mbsf)	Aromatic hydrocarbons (%)	Non-aromatic hydrocarbons (%)	Thiophenes (%)	Pyrroles (%)	HI (mg HC/g TOC)
157-955A-						
3H-7, 55-61	27.15	37.7	46.2	7.4	8.7	291
5H-2, 46-48	38.56	36.1	48.0	9.1	6.8	277
8H-6, 130-133	73.90	39.4	44.6	7.6	8.4	224
10H-2, 96-100	86.66	35.9	47.7	10.8	5.6	269
16H-7, 47-50	150.62	46.9	39.7	9.4	4.0	182
51X-1, 33-36	474.73	43.6	46.1	7.3	3.0	206
60X-3, 70-76	564.60	41.4	48.9	9.9	2.8	264
157-956A-						
11H-3, 79-83	95.39	37.0	51.5	5.9	5.6	255

Note: HI = hydrogen index.

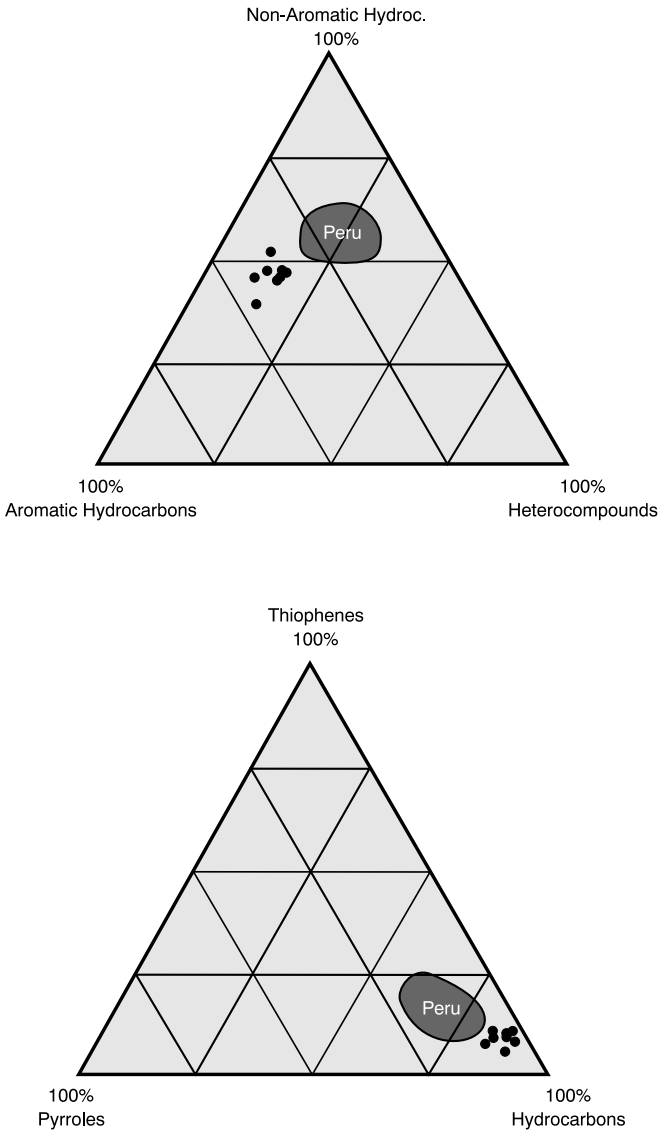

Figure 6. Results of the quantitation of individual compounds as revealed by pyrolysis-gas chromatography of samples from Sites 955 and 956, plotted in triangular diagrams of (**top**) aromatic and nonaromatic hydrocarbons and total heterocompounds and (**bottom**) total hydrocarbons, pyrroles, and thiophenes. Gaseous compounds are neglected. For comparison, the data established for the upwelling sediments off Peru are also shown (Lückge et al., 1996).

centages of aromatic hydrocarbons are nearly twice as high. These observations can be explained by favorable preservation conditions for labile marine organic matter in the upwelling areas, which allow a higher degree of preservation of heterocompounds.

Microscopically, four types of organic matter were distinguished: (1) structured marine particles (alginite), (2) unstructured organic matter of probable marine origin, (3) highly reflecting particles (inertinites and resedimented vitrinites), and (4) remains of higher land plants (vitrinites). Enumeration results for sediments from Site 955 are presented in Figure 7. The data indicate a rather high contribution of marine (structured and unstructured) organic matter for the upper 100 m of the sequence, below which the relative proportions of marine-derived organic matter are smaller but still on the order of 20%. This observation fits well with the distribution of HI values, which are smaller for the interval below 150 mbsf than for the sequence above. Vitrinites, which can be derived from the land plant vegetation of either northwest Africa or the Canaries, contribute between 15% and 35% to the organic particles in the upper 100 m. The relative contribution of vitrinites is greatest (45%–65%) for the samples from 150 and 177 mbsf and lowest (20%–25%) below 177 mbsf. Inertinites and resedimented vitrinites are concentrated below 300 mbsf and are least abundant between 35 and 100 mbsf. The latter observation may explain the rather high HI values established for this interval.

If compared to other deep marine sediments, the samples from Site 955 are enriched in marine-derived organic matter, but not to the same extent as upwelling sediments deposited closer to the continent. The respective average data for central-ocean sediments and upwelling sediments (based on the compilation from Littke and Sachsenhofer, 1994) are visualized in Figure 7. The samples from Site 955 plot in both fields. As the predominance of inertinites and resedimented vitrinites in most deep-sea sediments is explained by their high preservation potential compared to marine organic matter, the rather high contribution of marine organic matter in the sediments observed here indicates favorable preservation conditions.

According to microscopic observations and data, the maturity of the organic matter is low. Vitrinite reflectance values for the samples from the lower part of Hole 955A are ~0.3%. When compared with deep-sea sediments from hot areas, such as off the shore of Chile (Littke et al., 1995), these values indicate a low degree of thermal maturation. This is confirmed by the observation of strongly fluorescing liptinite macerals in UV-excited light.

Nonaromatic Hydrocarbons

Gas chromatograms of the nonaromatic hydrocarbon fractions of six selected samples from Site 955 are visualized in Figure 8. In all samples, a more or less bimodal distribution of the *n*-alkanes is observed. A pronounced concentration maximum is generally found at hentriacontane (C_{31}), and carbon preference index (CPI) values between 2.8 and 6.5 (Table 4) were determined. These high values are the result of a strong odd-over-even predominance, which is typical

of *n*-alkanes derived from cuticular waxes of vascular plants. The second concentration maximum of the bimodally distributed *n*-alkanes varies between C_{13} and C_{20}. For this range, a slight even-over-odd predominance is observed for some samples (e.g., Fig. 8D), although carbon preferences are not very pronounced. The *n*-alkane distributions found in samples from Site 955 could be explained by a mixed origin from allochthonous higher plant input and migration or from recycled organic matter of higher maturity.

On the other hand, a number of additional hydrocarbons are present in the elution range from C_{13} to C_{20}, which are especially abundant in the samples at 48.30 mbsf and 376.50 mbsf (Fig. 8C and 8E, respectively). This assemblage of compounds consists of alkenes, branched alkanes, and cycloalkanes (e.g., alkylcyclohexanes), as revealed by preliminary GC-MS investigations. Such compounds are usually not observed in high relative amounts in organic matter of higher thermal maturity. Hence, for these compounds, a direct input from marine biomass seems to be more probable than a contribution from migrated or recycled material. That methyl-branched alkanes are formed by various cyanobacteria has been known for a long time (e.g., Han et al., 1968; Gelpi et al., 1970). Recently, Kenig et al. (1995) presented a detailed characterization of the mono-, di- and trimethylalkane distribution in modern and Holocene cyanobacterial mats from Abu Dhabi. The authors assigned cyanobacteria as the source of the short-chain (C_{16}–C_{21}) branched alkanes, whereas long-chain (C_{24}–C_{45}) branched alkanes identified exclusively in the Holocene cyanobacterial mats were attributed to insect waxes. Because of the structural heterogeneity of the hydrocarbons identified in samples from Site 955 (i.e., *n*-alkanes, alkenes, branched alkanes, and cycloalkanes), an unequivocal assignment of the biological sources seems difficult. Our data, however, strongly suggest that a variety of organisms had contributed to the organic matter.

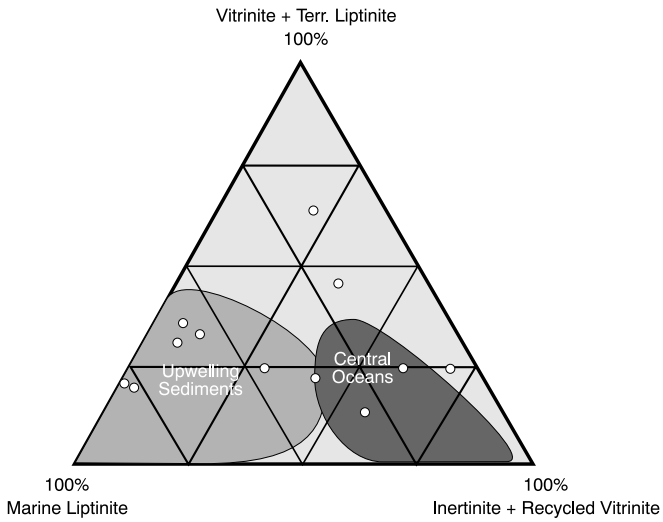

Figure 7. Petrographic composition of sedimentary organic matter at Site 955. For comparison, the main fields for "central oceans" and "upwelling sediments" (from Littke and Sachsenhofer, 1994) are also plotted.

Steroidal and triterpenoidal hydrocarbons, which are not very pronounced in samples from Site 955 (Fig. 8), are present in similar concentrations. The distribution patterns (Fig. 9) show some variation with depth that is related to diagenetic alteration and increasing maturity. The relative amounts of hopanes with the biological 17β, 21β-configuration (peaks 37, 43, and 51 in Fig. 9; Table 5) decrease, as compared with 17α,21β-hopanes (peaks 27, 33, 39, 40, etc., in Fig. 9; Table 5) and 17β,21α-moretanes (peaks 31, 42, etc., in Fig 9; Table 5). Fern-8-ene, fern-9(11)-ene and fern-7-ene (peaks 34, 35, and 41 in Fig. 9; Table 5) were detected in addition to the hopanoids. If identified in sediments, the latter are probably derived from bacteria rather than ferns (Brassell et al., 1981). These triterpenoids also show a maturity-related depth trend, with the thermally more stable fern-8-ene and fern-9(11)-ene becoming relatively enriched in comparison to the less stable fern-7-ene.

At 48.30 mbsf and 158.49 mbsf, sterenes and steradienes are predominant, whereas increasing amounts of steranes are observed at greater depths. This trend can be explained by the greater thermal maturity of the deeper samples. One C_{27}-, two C_{28}-, and two C_{29}-steradienes (peaks 7, 14, 19, 26, and 28 in Fig. 9; Table 5) all show similar mass spectrometric fragmentation patterns (base peak m/z 298), which is in agreement with Δ^5-unsaturation and an additional double bond at C-24 in the side chain (Rullkötter et al., 1982). These compounds are early diagenetic transformation products of sterols with unsaturated side chains, which are widespread in eucaryotic organisms. Among the sterenes, the Δ^2-unsaturated derivatives are predominant. The mass spectra of Δ^2-sterenes are characterized by a significant fragment ion at M^+-54 resulting from a loss of butadiene from the A-ring by a retro-Diels-Alder-fragmentation. The mass spectra of two isomers of 24-ethylcholest-2-ene (peaks 21 and 23 in Fig. 9; Table 5), shown in Figure 10, serve as examples. Extracted ion chromatograms for m/z 316, m/z 330, and m/z 344 in Figure 11 reveal the presence of at least four C_{27}-, six C_{28}-, and two C_{29}-isomers at a depth of 48.30 mbsf. Qualitatively similar, but quantitatively varying, distributions were found in all the samples analyzed. Our present observations are in contrast to most earlier publications on Δ^2-sterenes in marine sediments (e.g., Gagosian et al., 1978; Rullkötter et al., 1982; McEvoy and Maxwell, 1983), which reported only one isomer for each homologue. The occurrence of only two isomers of a given homologue would be explainable by the elimination of water from the corresponding 5α(H)- and 5β(H)-stanols (Mackenzie et al., 1982). However, this does not explain the occurrence of more than two Δ^2-sterenes, as observed for the C_{27}- and C_{28}-homologues. The reason for this finding remains unclear at present because the actual stereochemistry of the individual isomers is not known.

Fatty Acids

Distributions of free fatty acids were investigated for six selected samples from Site 955. Three representative gas chromatograms are shown in Figure 12. At 48.86 and 177.83 mbsf, the long-chain fatty

Table 4. Selected compound ratios, as determined by gas chromatography, of nonaromatic hydrocarbon fractions of selected samples from Site 955.

Core, section, interval (cm)	Depth (mbsf)	TOC (%)	CPI	LHCPI	Pr/*n*-C_{17}	Ph/*n*-C_{18}	Pr/Ph
157-955A-							
2H-2, 12-18	9.72	0.89	6.53	0.61	0.62	0.67	1.06
4H-4, 31-37	31.91	0.54	2.84	1.19	0.68	0.75	0.93
6H-2, 70-73	48.30	1.13	3.80	0.63	0.73	0.84	0.96
6H-4, 30-33	50.90	1.29	5.12	0.54	0.68	0.92	0.89
17H-6, 39-42	158.49	0.51	5.42	1.03	0.68	0.67	0.95
40X-6, 70-73	376.50	0.24	3.35	0.81	0.67	0.83	0.89
55X-3, 6-9	515.96	0.34	4.91	1.01	0.83	0.89	0.86
61X-1, 27-29	570.73	0.29	6.17	0.54	0.71	0.79	0.88
62X-7, 12-18	588.09	0.29	3.62	0.76	0.65	0.73	0.92

Note: CPI = $[(C_{27}+C_{29}+C_{31}+C_{33})/(C_{28}+C_{30}+C_{32}+C_{34})+(C_{27}+C_{29}+C_{31}+C_{33})/(C_{26}+C_{28}+C_{30}+C_{32})]/2$, LHCPI = $(C_{17}+C_{18}+C_{19})/(C_{27}+C_{28}+C_{29})$, Pr = pristane, and Ph = phytane.

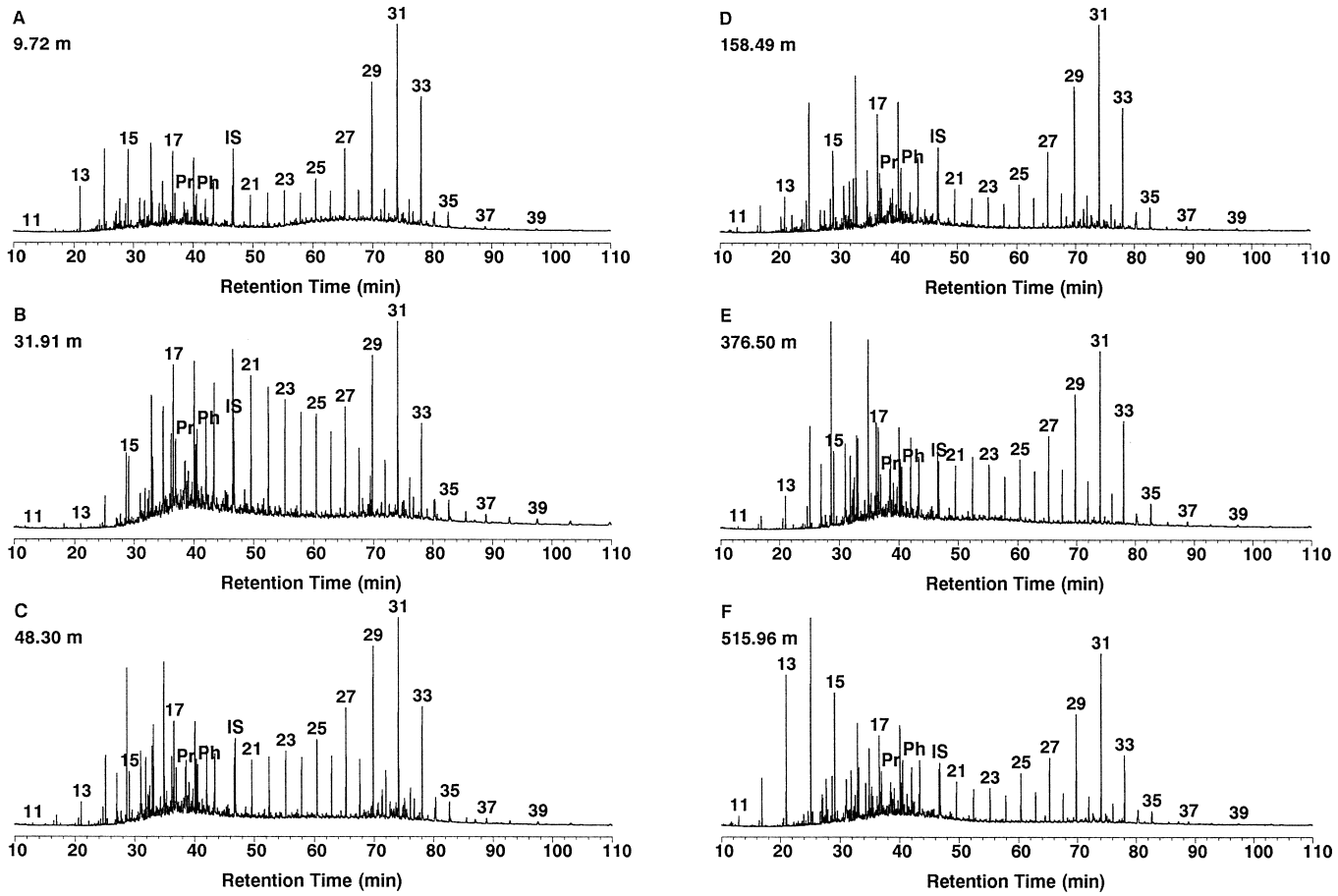

Figure 8. Gas chromatograms of the nonaromatic hydrocarbon fractions of selected samples from Site 955. **A.** Sample 157-955A-2H-2, 12–18 cm (9.72 mbsf). **B.** Sample 157-955A-4H-4, 31–37 cm (31.91 mbsf). **C.** Sample 157-955A-6H-2, 70–73 cm (48.30 mbsf). **D.** Sample 157-955A-17H-6, 39–40 cm (158.49 mbsf). **E.** Sample 157-955A-40X-6, 70–73 cm (376.50 mbsf). **F.** Sample 157-955A-55X-3, 6–9 cm (515.96 mbsf). Numbers = the chain length of *n*-alkanes. IS = internal standard (androstane). Pr = pristane and ph = phytane.

acids display a concentration maximum at C_{26}, which is typical for a higher plant input. Palmitic and stearic acids are very abundant, however, at variable ratios. These two acids are especially pronounced at greater depths. A high amount of these shorter chain fatty acids indicates a major input from algal and/or bacterial biomass without being of very high specificity. Only very low amounts of C_{16} and C_{18} unsaturated fatty acids were detected; this contrasts with other reports on fatty acid distributions in marine sediments (e.g., Smith et al., 1983; Hinrichs et al., 1995). On the other hand, Haddad et al. (1992) showed that unsaturated fatty acids are more rapidly depleted than saturated fatty acids in coastal marine sediments from Cape Lookout Bight. Significant amounts of the uncommon hexacosenoic acid (26:1), the origin of which is not clear, were found only at a depth of 48.86 mbsf, together with smaller amounts of tetracosenoic acid (24:1). Dehydroabietic acid, which is a typical constituent of resins, and hopanoic acids, which are diagenetic transformation products of certain bacterial lipids, were also detected in small amounts.

CONCLUSIONS

The Neogene sediments drilled south of Tenerife and Gran Canaria at Sites 955 and 956 are slightly enriched in organic matter, compared with average deep-sea sediments, whereas those drilled northeast of Gran Canaria at Site 954 contain only very low amounts of organic matter. This difference can be attributed to the redistribution of organic matter–rich upwelling sediments from the continental slope of northwest Africa (see Fig. 1). This redistribution strongly influenced sediment accumulation at Sites 955 and 956, as is evident from sedimentological features (Schmincke, Weaver, Firth, et al., 1995). Moreover, the highest organic carbon concentrations were observed in intervals affected by mass or turbidity currents. Obviously, redistribution of organic matter–rich sediments influenced sedimentation much less at the northern Site 954.

Organic matter composition is very heterogeneous at Sites 955 and 956. Clearly, marine-derived organic matter strongly contributes to the total organic matter. This strong contribution finds an expression in high percentages of marine liptinitic macerals (Fig. 7), in the presence of hydrocarbons and fatty acids indicative of algal and bacterial organic matter, and in surprisingly high HI values. The latter almost match those published for the upwelling sediments at the continental margin of northwest Africa (Fig. 6). This coincidence is regarded as an additional indication of a redistribution of these organic matter–rich continental margin deposits, favoring high contents and accumulation rates of organic carbon at the sites south of the Canary Islands.

In addition to the marine-derived organic matter, terrestrially sourced material is also present in vast amounts. Clear indications for the latter are the high CPI values for *n*-alkanes (Table 4; Fig. 8) and the microscopic data. It is tentatively assumed that a major source for this material is higher land plants on the Canary Islands, although vascular plants on the coasts of Morocco and Mauretania also may have provided material. The presence of resedimented organic matter derived from the erosion of older sedimentary rocks is documented

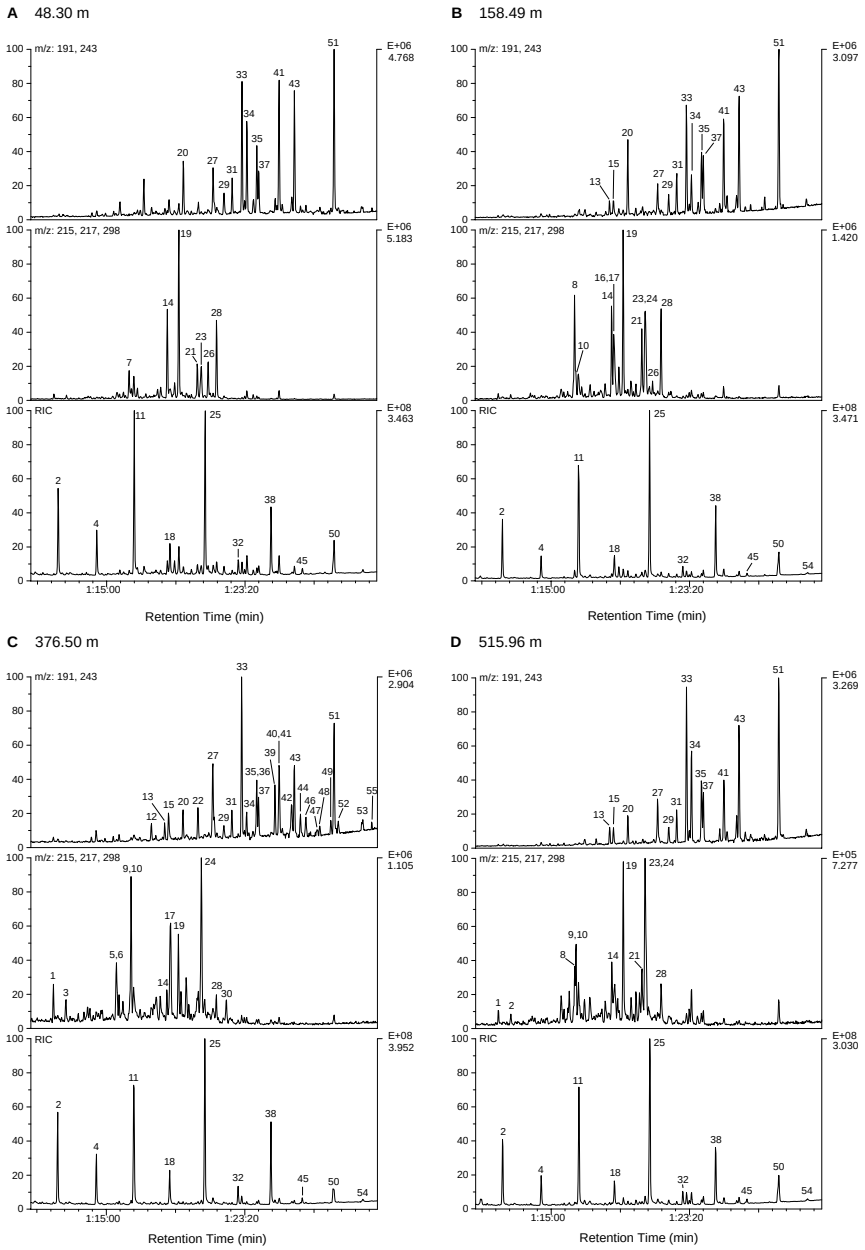

Figure 9. Partial reconstructed and extracted ion chromatograms of the nonaromatic hydrocarbon fractions of selected samples from Site 955. **A.** Sample157-955A-2H-2, 12–18 cm (48.30 mbsf). **B.** Sample 157-955A-17H-6, 39–40 cm (158.49 mbsf). **C.** Sample 157-955A-40X-6, 70–73 cm (376.50 mbsf). **D.** Sample 157-955A-55X-3, 6–9 cm (515.96 mbsf). The upper traces (sum of m/z 191 and m/z 243) represent triterpanes and triterpenes, the middle traces (sum of m/z 215, m/z 217, and m/z 298) represent steranes and sterenes. For peak identification, see Table 5.

by abundant inertinite and highly reflecting vitrinite and is attributed to erosion processes in northwest Africa.

The depositional conditions at Sites 954 and 955 were characterized by pelagic carbonate sedimentation, volcaniclastic deposition, and mass and turbidity flow sedimentation. Favorable conditions existed for the preservation of hydrogen-rich organic matter in high concentrations, especially during the mass and turbidity flow sedimentation. On average, Site 955 experienced such favorable conditions more often than Site 956, which is situated in a more distal position from the continent (Fig. 1). The reason for the preservation of organic matter in and under turbidite sediments is the rapid burial, which inhibited strong aerobic microbial decay at the sediment/water interface.

Maturation of organic matter clearly progresses with increasing depth at Site 955. Evidence for this progress is found mainly in the biological marker composition of nonaromatic hydrocarbons (i.e., in the compositional patterns of steroidal hydrocarbons and fernenes). On the other hand, extremely strong maturation, as earlier observed in oceanic sediments (e.g., at Site 859 close to the triple junction off the shore of Chile; Kvenvolden et al., 1995; Littke et al., 1995), can be excluded for the sites investigated here. This conclusion is in accordance with the low heat flow values of ~45 mW m^{-2} (Site 955) and 37 mW m^{-2} (Site 956) reported in the *Initial Reports* volume (Schmincke, Weaver, Firth, et al., 1995), which were estimated from in situ temperature measurements during Leg 157 operations. The high concentration of short-chain *n*-alkanes in the nonaromatic hydrocarbon fraction of the solvent extracts of some samples and of ethane in the headspace gas samples measured on board the *JOIDES Resolution* (Schmincke, Weaver, Firth, et al., 1995) indicates the migration of more mature hydrocarbons into the drilled upper section of the sedimentary column, rather than a strong maturation.

ACKNOWLEDGMENTS

We would like to thank W. Benders, U. Disko, F. Keller, W. Laumer, F. Leistner, A. Ropertz, H. Willsch, and especially Pr. Böttcher for technical support. Financial support by the Deutsche

Table 5. Peak identification for Figure 9.

Number	Compound
1	(20*S*)-13β(H),17α(H)-Diacholestane
2	*n*-Heptacosane
3	(20*R*)-13β(H),17α(H)-Diacholestane
4	*n*-Octacosane
5	(20*R*)-5α(H),14β(H),17β(H)-Cholestane
6	(20*S*)-24-Ethyl-13β(H),17α(H)-diacholestane
7	Cholesta-5,24-diene
8	Cholest-2-ene
9	(20*R*)-24-Ethyl-13β(H),17α(H)-diacholestane
10	5α(H),14α(H),17α(H)-Cholestane
11	*n*-Nonacosane
12	18α(H)-22,29,30-Trinorneohopane
13	22,29,30-Trinorhop-17(21)-ene
14	24-Methylcholesta-N,24-diene or 24-Methylcholesta-N,24(28)-diene
15	17α(H)-22,29,30-Trinorhopane
16	24-Methyl-2-cholestene
17	(20*R*)-24-Methyl-5α(H), 14α(H), 17α(H)-cholestane
18	*n*-Triacontane
19	24-Methylcholesta-N,24-diene or 24-Methylcholesta-N,24(28)-diene
20	17β(H)-22,29,30-Trinorhopane
21	24-Ethylcholest-2-ene
22	$C_{28}H_{48}$(M = 384,B = 191)
23	24-Ethylcholest-2-ene
24	(20*R*)-24-Ethyl-5α(H),14α(H),17α(H)-cholestane
25	*n*-Hentriacontane
26	24-Ethylcholesta-N,24-diene or 24-Ethylcholesta-N,24(28)-diene
27	17α(H)-30-Norhopane
28	24-Ethylcholesta-N,24-diene or 24-Ethylcholesta-N,24(28)-diene
29	Hop-17(21)-ene
30	(20*R*)-24-Propyl-5α(H),14α(H),17α(H)-cholestane
31	30-Normoretane
32	*n*-Dotriacontane
33	17α(H)-Hopane
34	Fern-8-ene
35	Fern-9(11)-ene
36	Moretane
37	17β(H)-30-Norhopane
38	*n*-Tritriacontane
39	(22*S*)-17α(H)-30-Homohopane
40	(22*R*)-17α(H)-30-Homohopane
41	Fern-7-ene
42	30-Homomoretane
43	17β(H)-Hopane
44	(22*S*)-17α(H)-30-Dihomohopane
45	*n*-Tetratriacontane
46	(22*R*)-17α(H)-30-Dihomohopane
47	(22*S*)-Dihomomoretane
48	(22*R*)-Dihomomoretane
49	(22*S*)-17α(H)-30-Trihomohopane
50	*n*-Pentatriacontane
51	17β(H)-30-Homohopane
52	(22*R*)-17α(H)-30-Trihomohopane
53	(22*S*)-17α(H)-Tetrahomohopane
54	*n*-Hexatriacontane
55	(22*R*)-17α(H)-Tetrahomohopane

Notes: Compounds are listed in elution order. Compound identification is based on relative retention times and mass spectral data.

Forschungsgemeinschaft (grant no. Li 613/1) is gratefully acknowledged. Last but not least, we thank K.-U. Hinrichs for his constructive review of an earlier draft of this manuscript.

REFERENCES

Berner, R.A., 1970. Sedimentary pyrite formation. *Am. J. Sci.*, 268:1–23.

————, 1984. Sedimentary pyrite formation: an update. *Geochim. Cosmochim. Acta*, 48:605–615.

Brassell, S.C., Wardroper, A.M.K., Thomson, I.D., Maxwell, J.R., and Eglinton, G., 1981. Specific acyclic isoprenoids as biological markers of methanogenic bacteria in marine sediments. *Nature*, 290:693–696.

Demaison, G., 1991. Anoxia vs. productivity: what controls the formation of organic-carbon-rich sediments and sedimentary rocks? *AAPG Bull.*, 75:499.

Durand, B., 1980. *Kerogen: Insoluble Organic Matter from Sedimentary Rocks:* Paris (Editions Technip).

Espitalié, J., Laporte, J.L., Leplat, P., Madec, M., Marquis, F., Paulet, J., and Boutefeu, A., 1977. Méthode rapide de caractérisation des roches mères, de leur potentiel pétrolier et de leur degré d'évolution. *Rev. Inst. Fr. Pet.*, 32:23–42.

Gagosian, R.B., and Farrington, J.W., 1978. Sterenes in surface sediments from the southwest African shelf and slope. *Geochim. Cosmochim. Acta*, 42:1091–1101.

Gelpi, E., Schneider, H., Mann, J., and Oró, J., 1970. Hydrocarbons of geochemical significance in microscopic algae. *Phytochemistry*, 9:603–612.

Haddad, R.I., Martens, C.S., and Farrington, J.W., 1992. Quantifying early diagenesis of fatty acids in a rapidly accumulating coastal marine sediment. *Org. Geochem.*, 19:205–216.

Han, J., McCarthy, E.D., Calvin, M., and Benn, M.H., 1968. Hydrocarbon constituents of the blue-green algae *Nostoc muscorum, Anacystis nidulans, Phormidium luridum and Chlorogloea fritischii. J. Chem. Soc. C*, 2785–2791.

Hinrichs, K.-U., Rullkötter, J., and Stein, R., 1995. Preliminary assessment of organic geochemical signals in sediments from Hole 893A, Santa Barbara Basin, offshore California. *In* Kennett, J.P., Baldauf, J.G., and Lyle, M. (Eds.), *Proc. ODP, Sci. Results*, 146 (Pt. 2): College Station, TX (Ocean Drilling Program), 201–211.

Katz, B.J., 1983. Limitations of "Rock-Eval" pyrolysis for typing organic matter. *Org. Geochem.*, 4:195–199.

Kenig, F., Sinninghe Damsté, J.S., Kock-van Dalen, A.C., Rijpstra, I.W.C., Huc, A.Y., and de Leeuw, J.W., 1995. Occurrence and origin of mono-, di-, and trimethylalkanes in modern and Holocene cyanobacterial mats from Abu Dhabi, United Arab Emirates. *Geochim. Cosmochim. Acta*, 14:2999–3015.

Kvenvolden, K.A., Rullkötter, J., Hostettler, F.D., Rapp, J.B., Littke, R., Disko, U., and Scholz-Böttcher, B., 1995. High-molecular-weight hydrocarbons in a south latitude setting off the coast of Chile, Site 859. *In* Lewis, S.D., Behrmann, J.H., Musgrave, R.J., and Cande, S.C. (Eds.), *Proc. ODP, Sci. Results*, 141: College Station, TX (Ocean Drilling Program), 287–297.

Littke, R., Disko, U., and Rullkötter, J., 1995. Characterization of organic matter in deep-sea sediments on the Chile continental margin with special emphasis on maturation in an area of high geothermal heat flow. *In* Lewis, S.D., Behrmann, J.H., Musgrave, R.J., and Cande, S.C. (Eds.), *Proc. ODP, Sci. Results*, 141: College Station, TX (Ocean Drilling Program), 119–132.

Littke, R., Rullkötter, J., and Schaefer, R.G., 1991. Organic and carbonate carbon accumulation on Broken Ridge and Ninetyeast Ridge, central Indian Ocean. *In* Weissel, J., Peirce, J., Taylor, E., Alt, J., et al., *Proc. ODP, Sci. Results*, 121: College Station, TX (Ocean Drilling Program), 467–489.

Littke, R., and Sachsenhofer, R.F., 1994. Organic petrology of deep sea sediments: a compilation of results from the Ocean Drilling Program and the Deep Sea Drilling Project. *Energy Fuel*, 8:1498–1512.

Lückge, A., Boussafir, M., Lallier-Vergès, E., and Littke, R., 1996. Comparative study of organic matter preservation in immature sediments along the continental margins of Peru and Oman. Part I: Results of petrographical and bulk geochemical data. *Org. Geochem.*, 24:437–451.

Mackenzie, A.S., Brassell, S.C., Eglinton, G., and Maxwell, J.R., 1982. Chemical fossils: the geological fate of steroids. *Science*, 217:491–504.

McEvoy, J., and Maxwell, J.R., 1983. Diagenesis of steroidal compounds in sediments from the southern California Bight (DSDP Leg 63, Site 467). *In* Bjoroy, M., *Advances in Organic Geochemistry:* Chichester (Wiley), 449–464.

McIver, R.D., 1975. Hydrocarbon occurrences from JOIDES Deep Sea Drilling Project. *Proc. Ninth Petrol. Congr.*, 269–280.

Meyers, P.A., 1992. Organic matter variations in sediments from DSDP sites 362 and 532: evidence of upwelling changes in the Benguela Current upwelling system. *In* Summerhayes, C.P., Prell, W.L., and Emeis, K.C. (Eds.), *Upwelling Systems: Evolution Since the Early Miocene.* Geol. Soc. Spec. Publ. London, 64:323–329.

Müller, P.J., and Suess, E., 1979. Productivity, sedimentation rate, and sedimentary organic matter in the oceans, I. Organic carbon preservation. *Deep-Sea Res. Part A*, 26:1347–1362.

Pedersen, T.F., and Calvert, S.E., 1990. Anoxia vs. productivity: what controls the formation of organic-carbon-rich sediments and sedimentary rocks? *AAPG Bull.*, 74:454–466.

Radke, M., Sittardt, H.G., and Welte, D.H., 1978. Removal of soluble organic matter from rock samples with a flow-through extraction cell. *Anal. Chem.*, 50:663–665.

Radke, M., Willsch, H., and Welte, D.H., 1980. Preparative hydrocarbon group type determination by automated medium pressure liquid chromatography. *Anal. Chem.*, 52:406–411.

Ruddiman, W., Sarnthein, M., Baldauf, J., et al., 1988. *Proc. ODP, Init. Repts.*, 108 (Sections 1 and 2): College Station, TX (Ocean Drilling Program).

Rullkötter, J., von der Dick, H., and Welte, D.H., 1982. Organic petrography and extractable hydrocarbons of sediment from the Gulf of California, Deep Sea Drilling Project Leg 64. *In* Curray, J.R., and Moore, D.G., *Init. Repts. DSDP,* 64: Washington (U.S. Govt. Printing Office), 837–853.

Sachsenhofer, R.F., and Littke, R., 1993. Vergleich und Bewertung verschiedener Methoden zur Berechnung der Vitrinitreflexion am Beispiel von Bohrungen des Steirischen Tertiärbeckens. *Zentralbl. Geol. Palaeontol.*, 1992/1:597–610.

Schlanger, S.O., and Jenkyns, H.C., 1976. Cretaceous oceanic anoxic events: causes and consequences. *Geol. Mijnbouw,* 55:179–184.

Schmincke, H.-U., Weaver, P.P.E., Firth, J.V., et al., 1995. *Proc. ODP, Init. Repts.*, 157: College Station, TX (Ocean Drilling Program).

Smith, D.J., Eglinton, G., and Morris, R.J., 1983. The lipid chemistry of an interfacial sediment from the Peru continental shelf: fatty acids, alcohols, aliphatic ketones and hydrocarbons. *Geochim. Cosmochim. Acta,* 47:2225–2232.

Stach, E., 1982. The macerals of coal. *In* Stach, E., et al. (Eds.), *Stach's Textbook of Coal Petrology:* Berlin (Gebr. Bornträger), 87–139.

Stein, R., and Littke, R., 1990. Organic-carbon-rich sediments and paleoenvironment: results from Baffin Bay (ODP-Leg 105) and the upwelling area off Northwest Africa (ODP-Leg 108). *In* Huc, A.Y. (Ed.), *Deposition of Organic Facies. AAPG Stud. in Geol.*, 30:41–56.

Stein, R., Rullkötter, J., Littke, R., Schaefer, R.G., and Welte, D.H., 1988. Organofacies reconstruction and lipid geochemistry of sediments from the Galicia Margin, Northeast Atlantic (ODP Leg 103). *In* Boillot, G., Winterer, E.L., et al., *Proc. ODP, Sci. Results*, 103: College Station, TX (Ocean Drilling Program), 567–585.

Stein, R., Rullkötter, J., and Welte, D.H., 1986. Accumulation of organic-carbon-rich sediments in the late Jurassic and Cretaceous Atlantic Ocean—a synthesis. *Chem. Geol.*, 56:1–32.

Stein, R., ten Haven, H.L., Littke, R., Rullkötter, J., and Welte, D.H., 1989. Accumulation of marine and terrigenous organic carbon at upwelling Site 658 and nonupwelling Sites 657 and 659: implications for the reconstruction of paleoenvironments in the eastern subtropical Atlantic through late Cenozoic times. *In* Ruddiman, W., Sarnthein, M., et al., *Proc. ODP, Sci. Results*, 108: College Station, TX (Ocean Drilling Program), 361–385.

Tissot, B.P., and Welte, D.H., 1984. *Petroleum Formation and Occurrence* (2nd ed.): Heidelberg (Springer-Verlag).

van Andel, T.H., Heath, G.R., and Moore, T.C., Jr., 1975. Cenozoic history and paleoceanography of the central equatorial Pacific Ocean: a regional synthesis of Deep Sea Drilling Project data. *Mem.—Geol. Soc. Am.*, 143.

Date of initial receipt: 8 July 1996
Date of acceptance: 28 April 1997
Ms 157SR-144

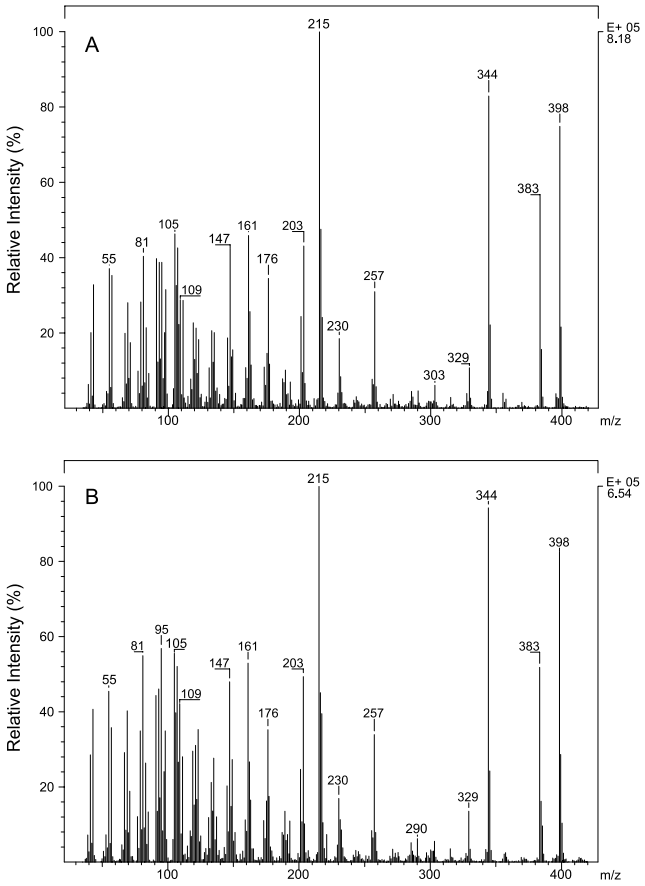

Figure 10. Mass spectra of two stereoisomers of 24-ethylcholest-2-ene. **A.** Scan 3084 of the nonaromatic hydrocarbon fraction of Sample 157-955A-6H-2, 70–73 cm (48.30 mbsf); peak 21 shown in Figure 9. **B.** Scan 3093 of the nonaromatic hydrocarbon fraction of Sample 157-955A-6H-2, 70–73 cm (48.30 mbsf); peak 23 shown in Figure 9.

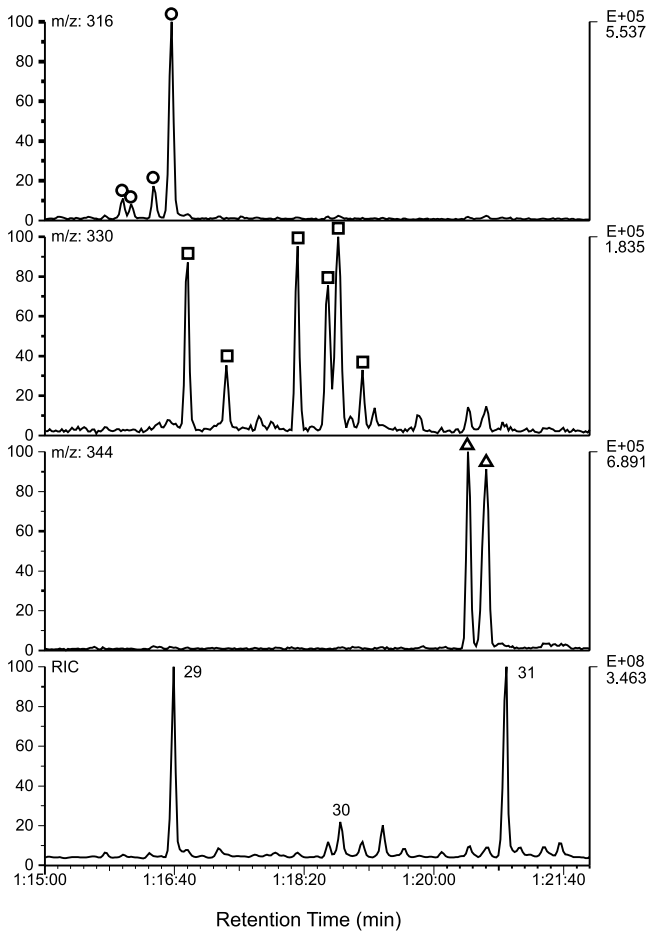

Figure 11. Partial reconstructed and extracted ion chromatograms of the non-aromatic hydrocarbon fractions of Sample 157-955A-6H-2, 70–73 cm (48.30 mbsf). Circles = cholest-2-enes (m/z 316), squares = 24-methylcholest-2-enes (m/z 330), triangles = 24-ethylcholest-2-enes (m/z 344), and numbers = the chain length of *n*-alkanes (RIC).

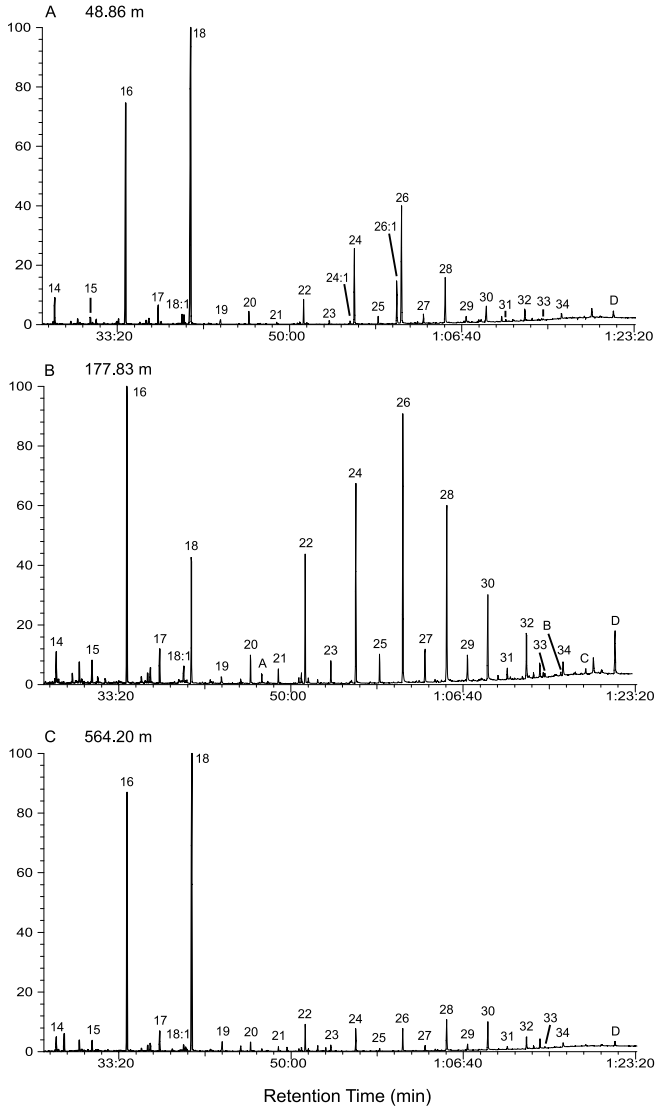

Figure 12. Partial reconstructed ion chromatograms of the methylated free fatty acid fractions of selected samples from Site 955. **A.** Sample 157-955A-6H-2, 126–130 cm (48.86 mbsf). **B.** Sample 157-955A-20X-1, 143–147 cm (177.83 mbsf). **C.** Sample 157-955A-60X-3, 30–34 cm (564.20 mbsf). Numbers indicate the chain length of *n*-fatty acids (16:1 = hexadecenoic acid; 18:1 = octadecenoic acid; 24:1 = tetracosenoic acid; 26:1 = hexacosenoic acid); A = dehydroabietic acid; B = dihomohop-17(21)-enoic acid; C = 17β,21β-homo-hopanoic acid; and D = 17β,21β-dihomohopanoic acid).

Prior Chapter Contents Next Chapter